J Mater Sci (2008) 43:2799–2805
DOI 10.1007/s10853-008-2543-z

The effect of nano-sized sintering aids on toughening behavior of silicon nitride

Sriharsha Pasupuleti · Ramseshu Peddetti · Sridhar Santhanam · Kei-Peng Jen · Zachary N. Wing · Joseph P. Halloran · Mathias Hecht

Received: 4 October 2007 / Accepted: 7 February 2008 / Published online: 28 February 2008

Abstract Processing plays an important role in determining the microstructure of silicon nitrides which in turn influences the mechanical properties, such as hardness and toughness. Sintering aids are an important processing parameter. The influence of the chemistry of sintering aids on properties of silicon nitrides is a well-explored subject. Here the size of sintering aids used and its impact on microstructure and mechanical properties is explored. Specifically the use of nano-scale versus micron-scale sintering aids is examined. Microstructures and mechanical properties for silicon nitrides hot-pressed with nano-sized sintering aids are compared with a reference silicon nitride hot-pressed with micron-sized sintering aids. Hardness and fracture toughness are determined at room temperature using hardness indents. Grain size and aspect ratio distributions are determined for the two silicon nitrides and their impact on mechanical properties are examined. Toughening behavior is studied by experimentally determining R-curves. Both toughness and toughening (R-curve) behavior are shown to improve with the use of nano-scale sintering aids.

Introduction

The favorable mechanical, physical, and chemical properties of silicon nitrides make them very desirable for a variety of applications. Their hardness and wear resistance make them suitable for bearing applications [1]. These bearing-grade silicon nitrides possess a microstructure with a mix of alpha and beta silicon nitride grains that simultaneously confers hardness and toughness. Silicon nitrides are used as cutting tool materials too [2]. Here the requirement is one of high fracture toughness which is achieved with a microstructure of entirely beta phase grains with an acicular morphology that leads to a self-reinforcing structure. Silicon nitride–silicon carbide nanocomposites have also been fabricated for cutting tool applications [3].

The mechanical behavior of liquid-phase sintered silicon nitrides is dictated to a large extent by their grain structure and the intergranular phase or film. The silicon nitride starting powder characteristics, the amount and type of sintering aids and secondary phase additives, and the sintering process parameters [4, 5] all play a role in affecting the microstructure. To obtain superior toughness and strength, a fine-grained microstructure with a high proportion of elongated beta grains is preferred [6, 7]. These in situ grown beta silicon nitride grains can significantly improve the fracture toughness over monolithic ceramics, producing self-reinforced silicon nitrides. Ex situ toughening of silicon nitrides is also accomplished with the addition of fibers such as SiC and Carbon [8–11].

The role that sintering aids play in determining the microstructure and properties of silicon nitrides has been studied extensively [12–15]. The impact of chemistry of sintering aids on the ensuing microstructure has been well documented. For instance, Park et al. [16] show that the addition of Yttria and Hafnia as sintering aids can result in elongated beta silicon nitride grains conferring additional fracture toughness. Strecker et al. [17] use a rare earth oxide mixture as a sintering additive and show a cost effective alternative to Yttria. However, the impact of the

S. Pasupuleti · R. Peddetti · S. Santhanam (✉) · K.-P. Jen
Mechanical Engineering Department, Villanova University, Villanova, PA, USA
e-mail: sridhar.santhanam@villanova.edu

Z. N. Wing · J. P. Halloran · M. Hecht
Advanced Ceramics Manufacturing, Tucson, AZ, USA

scale of sintering aids used, micron versus nano, on the resulting microstructure and mechanical behavior, particularly the toughening, has not been sufficiently explored and documented in the literature. Micron-scale sintering aids have conventionally been mixed with silicon nitride powder by techniques such as ball milling, planetary milling, or attrition milling. As the scale of both the sintering aid particle size and the silicon nitride powder size shrinks, these conventional techniques can at times lead to problems such as agglomeration and inhomogeneous distribution. This in turn can lead to imperfect densification and less than acceptable mechanical properties. However careful processing can prevent such agglomeration issues.

Several efforts have been directed toward using non-conventional routes to achieving homogeneous mixtures of nano-scale sintering aids with silicon nitride powders. Chemical routes that incorporate nano-sized aids in situ have been developed [18]. Wang et al. [18] report on the use of a low temperature combustion process that creates nano-scale Yttria and Alumina sintering aids in situ within silicon nitride powders. The process results in a homogeneous distribution of sintering aids leading to excellent densification. A similar process was used by Bondanini et al. [19] who used a chemical coprecipitation process to obtain a nanodispersed amorphous sintering aid dispersion among silicon nitride powder. Sintering aids chosen in the study were Lanthanum Oxide and Yttrium Oxide. Herrmann et al. [20] used a plasmachemical route to produce nano-scale silicon nitride powder coated with Yttria and Alumina sintering additives. The coating prevents further hydrolysis of the silicon nitride powder thus reducing oxygen content. They were able to demonstrate the formation of nanostructured silicon nitride from these coated powders. Similarly, Bellosi et al. [12] utilized nano-scale silicon nitride powders doped with sintering aids (Yttria and Alumina) by simultaneous vapor condensation using plasma technology.

Chemical processes to coat silicon nitride powders with the sintering aids can be expensive, time consuming, and not amenable to scale-up for industrial production. Moreover, they can be difficult to apply to nano-scale silicon nitride powders [12]. The alternative to these methods is to return to conventional milling to mix silicon nitride powders and nano-scale sintering additive powders. Choosing a suitable milling medium and an appropriate milling duration can reduce agglomeration and inhomogeneous mixture problems.

In this investigation, the impact of the scale of the sintering aids on the microstructure and resulting toughness and toughening of beta silicon nitrides is studied. Conventional ball milling is utilized to obtain a homogeneous mix of silicon nitride powders with sintering aid powders. A silicon nitride prepared with micron-scale sintering aids is compared with a silicon nitride prepared with nano-scale sintering aids. A quantitative analysis of the grain structure is conducted and the results of this analysis are correlated with the measured mechanical properties. A comparison of the toughening behavior is made by experimentally determining R-curves.

Experimental procedure

A "micron-sized" silicon nitride powder with a d_{50} of 0.7 μm (>90% α-silicon nitride, H.C. Starck) was utilized in preparing the samples. The reference silicon nitride powder batch with Micron-scale Sintering Aids (MSA) (average particle size = 0.7 microns) was prepared using the micron-sized silicon nitride powder and conventional micron-scale Al_2O_3, Y_2O_3, and ZrO_2 sintering aids. A second batch with Nano-scale Sintering Aids (NSA) was prepared using the micron-sized silicon nitride powder and nano-scale Al_2O_3, Y_2O_3, and ZrO_2 sintering aids (size range 20–40 nm). The weight fraction of sintering aids in the two batches were identical. The weight percent values of Al_2O_3, Y_2O_3, and ZrO_2 were 6, 4, and 1%, respectively. The powders were ball milled inside a polyethylene jar with IPA for 24 h. The slurries were dried and sieved through a 325 mesh screen. The powders were placed inside a graphite die and uniaxially hot-pressed under a nitrogen atmosphere at 1,750 °C for 1 h. A pressure of 30 MPa was applied.

The densities of the hot-pressed materials were measured in the usual way by the Archimedes principle. The hardness and toughness of the samples were measured using a macro Vickers hardness tester (LECO LV-100, LECO Corporation, St. Joseph, MI) with a load of 10 kgf used to make the indents. The toughness was calculated using the Anstis formula [21]. Four-point flexure tests were done in accordance with ASTM C-1161 to determine the bend strengths.

Toughening ability was determined by R-curve measurements which were performed on rectangular bars, machined to dimensions of 50-mm length, 4-mm width, and 3-mm depth. The tensile surface of each specimen was polished to a 1-micron diamond finish. Three uniformly spaced indentations were placed on the tensile surface of each specimen with an indentation load of 196 N (20 Kgf). Care was taken to ensure one set of radial cracks at each indentation was perpendicular to the tensile stress direction in bending. After indentation, each of the samples was annealed at 1,000 °C for an hour in a flowing nitrogen atmosphere to eliminate residual stresses. Samples were loaded in a four-point bend fixture with an inner span of 20 mm and outer span of 40 mm. Loading was performed in a servohydraulic machine (MTS 810, MTS Systems Corporation,Eden Prairie, MN) under displacement control with a low crosshead speed of 0.05 mm/min. The sample was

incrementally loaded by small load increments to achieve stable crack propagation. Once the desired load level was achieved, the load was held for about 20 s before being quickly released. After each load step the increase in crack length (Δc) was measured. The loading arrangement was specially designed to generate a very stiff loading geometry.

Crack growth resistance, K_R, was plotted against the half surface crack length, c, to produce the R-curves. The crack growth resistance, K_R, is the maximum applied stress intensity factor at the tip of the indentation crack for each loading–unloading cycle.

$$K_R = Y\sigma\sqrt{c} \tag{1}$$

Here, σ is the peak bending stress in each loading–unloading cycle. The shape (geometry) factor, Y, is calculated using the empirical equation of Newman and Raju [22] and the procedure described in [23] for determining the ellipticity ratio of the crack. Loading–unloading cycles were continued until the specimen fractured.

Ramachandran and Shetty [24] proposed the following function for modeling experimental R-curves.

$$K_R = K_\infty - (K_\infty - K_0)\,\exp\left\{\frac{-(c - c_0)}{\lambda}\right\} \tag{2}$$

Here K_∞ and K_0 are the upper and lower bound crack growth resistances for the long and short crack limits, while λ is a crack-length normalizing parameter. This model provides useful parameters to characterize the R-curves and is used to model the experimental R-curves for the MSA and NSA silicon nitrides.

Specimens for microstructure characterization were polished and etched. Etching was performed with a gas mix of 8% O_2–92% CF_4 in a plasma etcher (Plasma Prep II, Structure Probe Inc., West Chester, PA). Microstructures of etched specimens were imaged using a Field Emission Scanning Electron Microscope (Hitachi S-4800-1, Hitachi HTA, Pleasanton, CA)). SIMAGIS Smart Imaging Spreadsheet (Smart Imaging Technologies, Houston, TX) was used to calculate grain size and aspect ratio distributions. Fracture surfaces were directly observed in the Scanning Electron Microscope. Powder diffractometry was performed using a Philips Powder Diffractometer (Philips PW1050, PANalytical Inc., Natick, MA) to ascertain phases in the specimens.

Results and discussion

Densities of the reference silicon nitride (MSA) and the NSA materials are shown in Table 1. Near theoretical density was achieved for both MSA and NSA silicon nitrides. Clearly, the use of nano-scale sintering aids has not hampered the densification of the NSA silicon nitride.

Table 1 Densities of MSA and NSA silicon nitrides

Specimen	Relative density (%)
MSA	99.7 ± 0.8
NSA	99.6 ± 0.2

Average HV10 hardness and toughness for these materials are reported in Table 2. While the hardness of the two materials are about the same, the toughness of the material with nano-sintering aids (NSA) is clearly superior. The toughness results were based on the size of the indentation cracks and were calculated using the Anstis formula [21]. The superior toughness is related to the microstructures exhibited by this material as will be described later. Four-point bend strengths are reported in the same table. A significant difference was observed in the flexure strength of MSA and NSA samples. The four-point bend strength was found to be 17% higher in samples prepared with nano-sized sintering aids.

Figure 1 shows the X-ray diffraction pattern from the NSA material. The dominant phase is β silicon nitride. There are no signs of any α peaks. It is clear that the α to β transformation has been completed. The diffraction pattern from the reference MSA material (Fig. 2) too shows the same β silicon nitride peaks, and therefore the MSA material too has undergone the complete transformation.

Table 2 HV10 macro Vickers hardness, indentation toughness, and bend strengths

Specimen	Hardness (GPa)	Toughness ($MPa\sqrt{m}$)	4-point bend strength (MPa)
MSA	15.0 ± 0.2	5.5 ± 0.4	884 ± 44
NSA	15.1 ± 0.2	7.2 ± 0.9	1038 ± 17

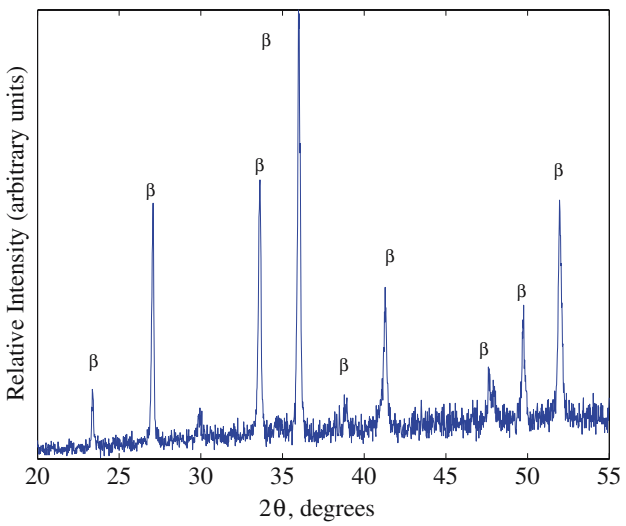

Fig. 1 X-ray diffraction pattern for the NSA silicon nitride shows β silicon nitride peaks

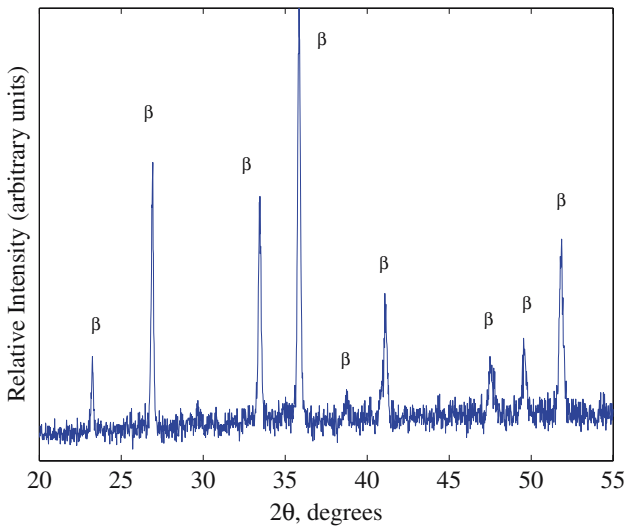

Fig. 2 X-ray diffraction pattern for the reference MSA silicon nitride shows β silicon nitride peaks

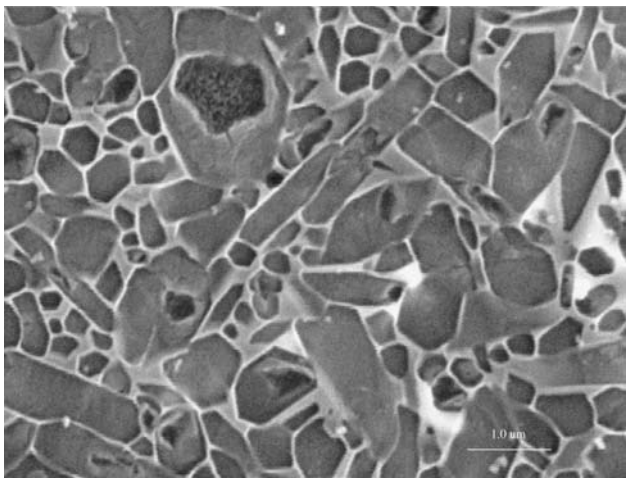

Fig. 3 Microstructure of the MSA silicon nitride

Microstructures of the reference MSA and the NSA silicon nitrides are shown in Figs. 3 and 4, respectively. Each of these microstructures shows characteristic beta silicon nitride grains with acicularity. Quantitative grain size (average diameter) and aspect ratio (major diameter/minor diameter) distributions were determined for these microstructures. More than 1,000 grains were used to compile statistics for each of the microstructures. The histograms of grain size distributions for the MSA and NSA silicon nitrides are shown in Fig. 5. The NSA silicon nitride shows a measurable increase in the numbers of grains of average diameter 0.2 microns and smaller in comparison to the reference MSA silicon nitride. Figure 6 presents the grain aspect ratio (major diameter/minor diameter) distributions in the two microstructures. Again, NSA shows a slightly higher fraction of grains of aspect ratio 2.0 and higher in comparison to the reference MSA.

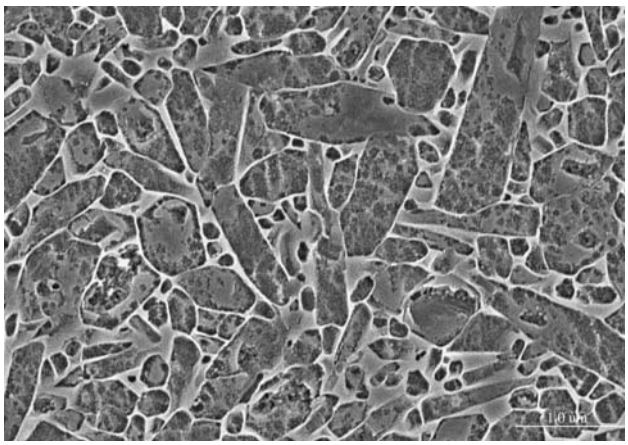

Fig. 4 Microstructure of the NSA silicon nitride

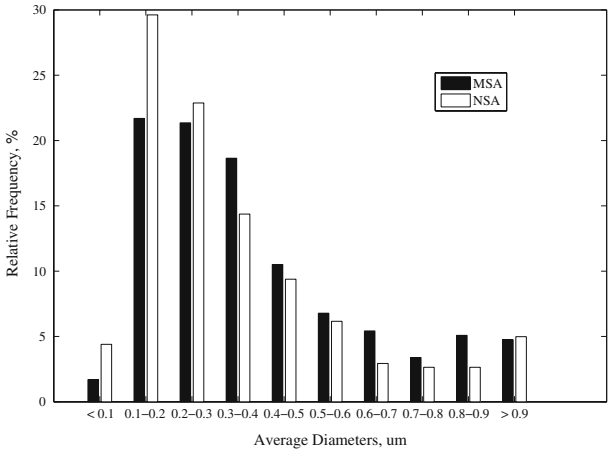

Fig. 5 Grain size (average grain diameter) distributions for the NSA and MSA silicon nitrides

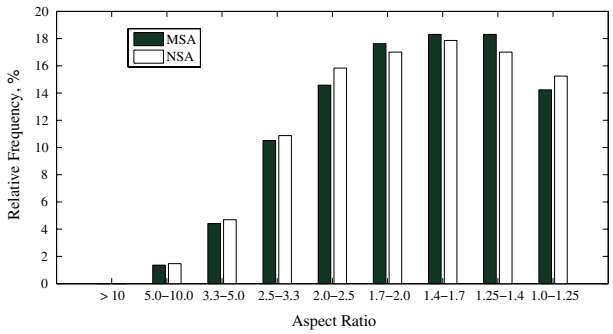

Fig. 6 Grain aspect ratio (major diameter/minor diameter) distributions for the NSA and MSA silicon nitrides

These would be the acicular grains that potentially contribute to toughness and toughening, giving rise to a self-reinforcing microstructure.

The use of nano-sintering aids has caused some refinement in the grain structure. Their use has increased the fraction of acicular grains marginally and has also caused an increase in the number of fine (low average-diameter,

0.2 microns and less) grains. These silicon nitrides densify by a liquid phase sintering mechanism, wherein the sintering aids combine with the silica on the surface of the silicon nitride powders and form a eutectic melt that facilitates particle rearrangement and solution-reprecipitation processes. Nano-scale sintering aids tend to be more active and melt at lower temperatures. As a result the liquid phase exists over a wider temperature range and a more prolonged time duration. Also because of the smaller size of nano-scale sintering aids in relation to micron-scale sintering aids, the ball milling process should produce a more homogeneous distribution of the nano-scale sintering aids. Hence the liquid phase in a silicon nitride with nano-scale sintering aids should be more homogeneously distributed thus providing a uniform distribution of sites for solution-reprecipitation processes. These factors should lead to a refinement of grain structure with the NSA silicon nitride exhibiting more numerous fine grains as well as more acicularity in the grain aspect ratios in comparison to the MSA silicon nitride.

The refinement in the microstructure of the NSA silicon nitride contributes to its improved fracture toughness (Table 2) as measured by the Vickers Indentation method. The increased presence of acicular grains and their distribution in a fine-grained matrix in the microstructure is a contributing cause to a self-reinforcement effect. The higher strength of the NSA silicon nitride (Table 2) could also be attributed to this refined grain structure. While the grain structure plays an important role in influencing mechanical properties, another key variable is the nature of the intergranular phase or film in liquid-phase sintered silicon nitrides. The chemistry and thickness of this intergranular film affects its strength, thereby influencing the strength and toughness of the silicon nitride. A number of studies have looked at the effect of the strength of this film and its role in influencing intergranular fracture. However, the role of the intergranular film in influencing the properties of the NSA silicon nitride is not considered here.

Figure 7 shows R-curves for the NSA material. Results are reported for three different test specimens of the same material. From the graphs it is evident that NSA exhibits classic toughening behavior. The K_R–c relationship of Eq. 2 was fit to the experimental results for NSA using a nonlinear least-squares method. These curvefits are shown in Fig. 7. The Ramachandran and Shetty [24] parameter values for the curve fits are shown in Table 3. NSA shows classic toughening curves with an initial steep increase in crack growth resistance with crack length followed by the development of a plateau. R-curves for the reference MSA silicon nitride are shown in Fig. 8. Parameters for the curvefits based on Eq. 2 are shown in Table 3. Again, three specimens of the MSA material were tested. While the MSA silicon nitride shows classic toughening behavior as well, the plateaus of the R-curves of MSA are lower than those of NSA. Evidence of this is also seen in the K_∞ values seen in Table 3. The average K_∞ value for the NSA

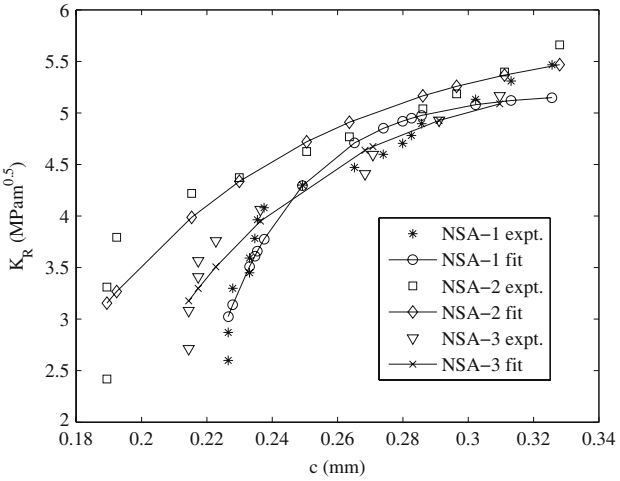

Fig. 7 Experimental R-curves for the NSA silicon nitride and curve fits based on Eq. 2

Table 3 Ramachandran and Shetty [24] parameters for MSA and NSA silicon nitrides

Specimen	K_∞ (MPa$\sqrt{m}$)	K_0 (MPa$\sqrt{m}$)	c_0 (mm)	λ (mm)
MSA-1	4.86	2.48	0.22	0.021
MSA-2	4.96	2.48	0.20	0.03
MSA-3	5.06	2.51	0.20	0.056
NSA-1	5.2	2.47	0.22	0.026
NSA-2	5.83	2.52	0.18	0.070
NSA-3	5.50	2.49	0.20	0.054

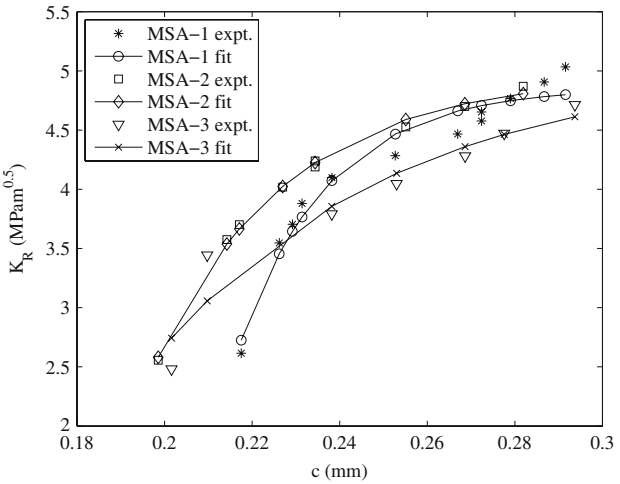

Fig. 8 Experimental R-curves for the MSA silicon nitride and curve fits based on Eq. 2

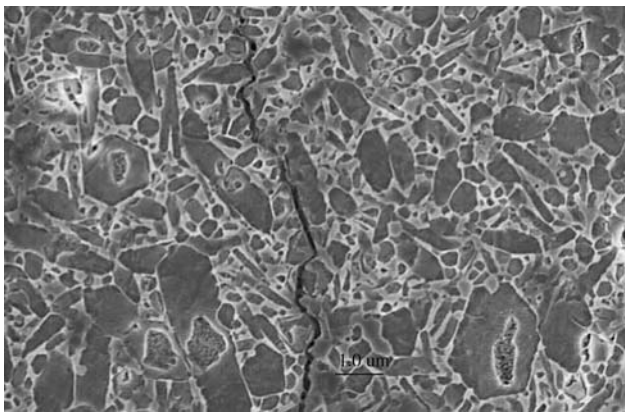

Fig. 9 Crack propagation through the grain structure of the NSA silicon nitride

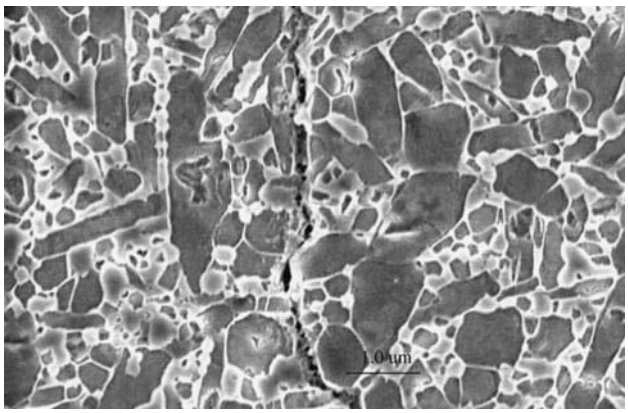

Fig. 10 Crack propagation through the grain structure of the MSA silicon nitride

silicon nitride is 5.51, while the corresponding value for the MSA silicon nitride is 4.96, an increase of about 11%. This is consistent with the findings on the indentation fracture toughness reported in Table 2. There is no discernible difference in the remaining parameters of Table 3 between the two materials.

Crack propagation paths were established for NSA. These cracks emanated from the additional indentations placed on the R-curve test bars, adjacent to the fracture-causing indentation crack. The fractured piece of the R-curve bar, containing this additional indentation, was plasma etched to reveal the grain structure surrounding the grown, subcritical indentation crack. Figure 9 shows crack propagation paths in NSA. There is clear evidence of crack-path deflection in NSA as a toughening mechanism. This deflection mechanism of toughening is due to the presence of acicular grains. A similar mechanism is seen in Fig. 10 for the MSA silicon nitride. The refined microstructure of NSA should promote crack-path deflection as a toughening mechanism.

Conclusions

The role of the scale of the sintering aids on the resulting microstructure and toughening behavior of hot-pressed silicon nitrides has been studied. Silicon nitrides prepared with nano-scale sintering aids were compared with silicon nitrides with micron-scale sintering aids. Conventional ball milling was used to disperse the sintering aids. Microstructure analysis indicates that the use of nano-scale sintering aids has caused a refinement of the microstructure when compared with micron scale aids. The NSA material has a finer grain size as well as a marginally increased acicularity of grain shapes. Densification is not negatively impacted by the use of the nano-scale sintering aids. In fact, near theoretical density was achieved for both MSA and NSA materials. There is little change in hardness but a significant gain in toughness and strength due to the nano-scale sintering aids. Silicon nitride with nano-scale sintering aids shows a classic toughening (R-curve) behavior with a sharp rise in the crack growth resistance with crack length followed by a plateau. The plateaus achieved with the NSA material are higher than for the MSA silicon nitride, indicative of the fact that nano-scale sintering aids are improving toughening behavior. Crack propagation paths through the microstructure of both NSA and MSA silicon nitrides show that crack-path deflection is the dominant toughening mechanism in both.

Acknowledgements The Office of Naval Research supported this research through Contract Number: N00014-05-C-0331. A Major Research Instrumentation award (Award Number 0521011) from the National Science Foundation supported the acquisition of the high resolution scanning electron microscope.

References

1. Liu M, Nemat-Nasser S (1999) Percolation of single-walled carbon nanotubes in ceramic matrix nanocomposites. J Mater Res 14(12):4621
2. Huang CZ, Li M, Wang SL, Sun J, Liu HL, Ai X (2004) A study on a self-toughening silicon nitride ceramic tool and its cutting performance. Key Eng Mater 259–260:37
3. Sajgalik P, Hnatko M, Lences Z, Dusza J, Kasiarova M (2004) In situ preparation of silicon nitride-silicon carbide nanocomposites for cutting tool applications. Int J Appl Ceram Technol 259–260:37
4. Riley Frank L (2000) Silicon nitride and related materials. J Am Ceram Soc 83(2):245
5. Ziegler G, Heinrich J, Wotting G (1987) Review relationships between processing, microstructure, and properties, of dense and reaction-bonded silicon nitrides. J Mater Sci 22:3041
6. Coutinho ACS, Bressiani JC, Bressiani AHA (2003) Influence of microstructural characteristics on the mechanical properties of silicon nitride with yttria, alumina, and neodymia sintering aids. Mater Sci Forum 416–418:567
7. Dave Carruthers W, Becher PF, Ferber MK, Pollinger J (2002) Advances in the development of silicon nitride and other

ceramics. Proceedings of ASME Turbo Expo 2002, GT-2002-30504, pp 1–10
8. Bhatt RT, Hull DR, Eldridge JI, Babuder R (2002) Effects of interface coating and nitride enhancing additive on properties of hi-nicalon sic fiber reinforced reaction bonded silicon nitride composites. J Mater Sci 37:141
9. Go P, Sung C, Kostetsky JJ, Vasilos T (2002) Silicon nitride matrix composites with unidirectional silicon carbide whisker reinforcement. J Mater Sci 37:2587
10. Wang C, Huang Y, Xie Z (2001) Improved resistance to damage of silicon carbide whisker reinforced silicon nitride matrix composites by whisker oriented alignment. J Am Ceram Soc 84(1):161
11. Hyuga H, Jones MI, Hirao K, Yamauchi Y (2005) Friction and wear properties of sin/carbon fiber composites with aligned microstructures. J Am Ceram Soc 88(5):1239
12. Bellosi A, Vicens J, Medri V, Guicciardi S (2005) Nanosize silicon nitride: characteristics of doped powders and of the related sintered materials. Appl Phys A Mater Sci Process 81:1045
13. Strecker K, Gonzaga R, Ribiero S, Hoffmann M (2000) Substitution of yttria by a rare earth oxide mixture as sintering additive of silicon nitride ceramics. Mater Lett 45:39
14. Goto Y, Thomas G (1995) Microstructure of silicon nitride ceramics sintered with rare earth oxides. Acta Metall Mater 43(3):923
15. Hoffmann MJ (1995) Relationship between microstructure and mechanical properties of silicon nitride ceramics. Pure Appl Chem 67(6):939
16. Park D-S, Lee S-Y, Kim H-D, Yoo B-J, Kim B-A (1998) Extra large grains in the silicon nitride ceramics doped with yttria and hafnia. Journal of the American Ceramic Society 81(7):1876
17. Strecker K, Gonzaga R, Ribeiro S, Hoffmann MJ (2000) Substitution of yttria by a rare earth oxide mixture as a sintering additive for silicon nitride ceramics. Mater Lett 45:39
18. Wang L, Sigmund WM, Roy S, Aldinger F (1999) Improved densification by nano-sized sinering aids for silicon nitride. J Mater Res 14:4562
19. Bondanini A, Monteverde F, Bellosi A (2001) Influence of powder characteristics and powder processing routes on microstructure and properties of hot pressed silicon nitride materials. J Mater Sci 36:4851
20. Herrmann M, Schulz I, Zalite I (2004) Microstructural evolution and mechanical properties of silicon nitride with ytterbia as a sintering additive. J Eur Ceram Soc 24:3327
21. Anstis GR, Chanticul P, Lawn BR, Marshall DB (1981) A critical evaluation of indentation techniques for measuring fracture toughness: I direct crack measurements. J Am Ceram Soc 4(9):538
22. Newman JC, Raju IS (1981) An empirical stress intensity factor equation for the surface crack. Eng Fract Mech 15(1):185
23. Gong J, Guan Z (2000) Crack location dependent r-curve behavior in silicon nitride. J Eur Ceram Soc 20:1339
24. Ramachandran N, Shetty DK (1991) Rising crack growth resistance (r-curve) behavior of toughened alumina and silicon nitride. J Am Ceram Soc 74:2634